Engineering Science and Technology, an International Journal xxx (2017) xxx–xxx

HOSTED BY

Contents lists available at ScienceDirect

Engineering Science and Technology, an International Journal

journal homepage: www.elsevier.com/locate/jestch

Full Length Article

Dynamic performance improvement of standalone battery integrated PMSG wind energy system using proportional resonant controller

Dileep Kumar Varma Sagiraju [a,*], Obulesu Y.P. [b], Sai Babu Choppavarapu [c]

[a] Department of Electrical and Electronics Engineering, Shri Vishnu Engineering College for Women (A), Vishnupur, Bhimavaram 534 202, Andhra Pradesh, India
[b] School of Electrical Engineering, VIT University, Vellore, Tamilnadu, India.
[c] Department of Electrical Engineering, University College of Engineering Kakinada (A), JNTUK, Kakinada, Andhra Pradesh, India

ARTICLE INFO

Article history:
Received 28 November 2016
Revised 16 March 2017
Accepted 20 March 2017
Available online xxxx

Keywords:
PMSG
Proportional resonant (PR) controller
Battery energy controller
Power quality
Power management

ABSTRACT

The load voltage and frequency should be controlled under steady state and transient conditions in off grid applications. Power quality and power management is very important task for rural communities under erratic wind and load conditions. This paper presents a coordinated Proportional resonant (PR) and battery energy controller for enhancement of power quality and power management in direct drive standalone wind energy system. The dynamic performance of standalone direct drive Permanent Magnet Synchronous Generator (PMSG) is investigated with the proposed control scheme under various operating conditions such as fluctuating wind with step increase and decrease in wind velocity, balanced and unbalanced load conditions. The proposed PR control strategy with battery energy controller also ensures effective power balance between wind and battery source in order to fulfill the load demand. The superiority of the proposed control strategy is confirmed by comparing with the traditional vector control strategy under fluctuating wind and load conditions through MATLAB/SIMULINK platform.

1. Introduction

The fast exhaustion of fossil fuels and environmental concerns motivated the researchers to pay more attention on the alternate energy sources. Among all renewable energy resources, wind energy system has been treated as one of the greatest potential and rapid expanding alternate energy sources to fulfil the global load demand [16]. The contribution of wind energy is about 30% of total installed capacity of renewable energy sources globally. Wind turbines are usually operational either with fixed speed or variable speed generators. At present, variable speed wind generators are widely used in wind energy application because of their various advantages over fixed speed wind generators. Variable speed wind turbines can be either doubly fed induction generator or permanent magnet synchronous generators. The permanent magnet wind generator is emerging as the best alternative for the stand alone applications because of its various advantages like simple in construction, less maintenance due to the absence of gear box, high efficiency, more power density, better power factor and absence of dc excitation [1,20]. Hence, PMSG is proved to be viable for rural communities where grid electricity is not accessible. Majority of rural communities are still using diesel generators. However, due to the high fuel cost and environmental concern, diesel generators can be replaced with PMSG.

The voltage and frequency control at load and machine terminals of standalone PMSG wind energy system is a critical task under unsteady wind and load conditions. The variability in wind profile results in variation in machine torque, DC link voltage, rotor speed, output voltage and frequency excursions. Power sharing between wind and battery source in order to meet the required load demand is very important under variable wind and load conditions. Under these circumstances, the battery energy storage system can be embedded with PMSG to flatten the wind turbine output power as well as to improve power management in standalone system.

Various control strategies are reported in literature for the amelioration of power quality and power management in standalone wind energy system. The authors have reported on vector PI control strategy in dq reference frame for load side converter to improve power quality for standalone PMSG under variable wind and load conditions [12,11,10,17,19,30]. The authors [21,22] have proposed vector control strategy for standalone battery integrated wind energy system for improving quality of power as well as

* Corresponding author.
E-mail addresses: varma8332@gmail.com (D.K.V. Sagiraju), ypobulesh@gmail.com (Y.P. Obulesu), chs_eee@yahoo.co.in (S.B. Choppavarapu).
Peer review under responsibility of Karabuk University.

http://dx.doi.org/10.1016/j.jestch.2017.03.010
2215-0986/

power management. However, these control strategies are effective under balanced linear loads and ineffective with unbalanced loads. In all the aforementioned control strategies, SRF (Synchronous Reference Frame) PLL is utilized to extract the phase angle of load voltage under balanced and unbalanced grid conditions. However, SRF PLL works well for balanced load conditions and is not satisfactory under unbalanced load conditions. When load voltage becomes unbalanced, the negative sequence voltage component creates double frequency oscillations in the generator torque, and developes high stress in mechanical drive train system. In this unbalanced condition, proper synchronization with load voltage and accurate and precise information is required for the controller. Hence, to mitigate the negative sequence effect due to unbalanced loads, the authors [25,26] proposed dual vector control strategy for standalone wind energy system. The dual vector control scheme can be implemented in dual positive and negative reference frames to extract both positive as well as negative sequence components from an unbalanced load voltage vector. However, the disadvantage of decomposition of load quantities into sequence components involves complex transformations, which in turn introduce the time delay that affects the controller performance.

The authors [14,23,34,24] presented fuzzy and predictive control schemes to improve the dynamic performance of standalone PMSG under variable wind and load conditions. However, these control schemes are not effective under unbalanced load conditions. Under unbalanced load conditions, the Fuzzy and predictive controller have to be realized in two synchronous reference frames to extract the positive and negative sequence components separately. Moreover, the complexity as well as the computational burden on the controller increases. To overcome these problems and to upgrade the system performance, the authors [4,13,29,28,27,18,33] have proposed proportional resonant control to improve the dynamic response for DFIG (Doubly Fed Induction Generator) wind energy system under balanced, unbalanced and distorted conditions. However, in the above mentioned literature, the authors have focussed only on power quality issues and not considered power management and reliability aspects. Hence, this paper explores a coordinated proportional resonant and battery energy controller for standalone battery integrated PMSG to enhance power quality and power management under variable wind and load conditions. The efficacy of the proposed control approach is manifested by analysing with the typical vector control strategy using Matlab/Simpower system.

The paper is formulated as follows. Section 2 explicates the wind turbine and PMSG modeling. The proposed test system and the proposed control scheme is discussed in Section 3. Section 4 elucidates the result analysis and finally Section 5 draws conclusion.

2. Wind turbine and PMSG modeling

2.1. Wind turbine modeling

The wind turbine power at any wind speed is given by [5]

$$P_t = \frac{1}{2}\rho A v_w^3 \times C_p(\lambda,\beta) \tag{1}$$

where A is swept area covered by turbine blade (in m^2), C_p is wind turbine power coefficient as a function of tip speed ratio λ and pitch angle β (in degrees), ρ is air density factor in (kg/m^3), V_w is wind speed (in m/s).

The turbine power mainly depends on various factors such as maximum power coefficient, air density factor, swept area of blades and wind speed .The power extraction from wind turbine also depends on turbine hub height as the wind speed tends to be higher as height increases from ground level.

The tip speed ratio of wind turbine is given by [6]

$$TSR = \lambda_{OPT} = \frac{\omega_m R}{v_w} \tag{2}$$

where ω_m is the machine angular speed (in rad/s), R is turbine blade radius (in m).

Substituting v_w from (2) into (1), the wind turbine output power can be written as

$$P_t = 0.5\rho A C_p \left(\frac{\omega_m R}{\lambda}\right)^3 \tag{3}$$

2.2. PMSG modeling

This subsection is devoted to explain about the mathematical modelling of PMSG in dq-reference frame. The *dq0* Park's transformation is used to simplify the analysis of synchronous machinery models, and was first introduced by R. H. Park [8]. The mathematical model of the PMSG is related to the classical synchronous machine. The PMSG is modeled with an assumption of sinusoidal-distributed windings and neglecting saturation, eddy currents, and hysteresis losses [9]. By Applying park transformation, the PMSG stator voltage from the abc to dq0 conversion is written as

$$\begin{bmatrix} V_d \\ V_q \\ V_0 \end{bmatrix} = \sqrt{\frac{2}{3}} \begin{bmatrix} \cos\theta_r & \cos\left(\theta_r - \frac{2\pi}{3}\right) & \cos\left(\theta_r + \frac{2\pi}{3}\right) \\ -\sin\theta_r & -\sin\left(\theta_r - \frac{2\pi}{3}\right) & -\sin\left(\theta_r + \frac{2\pi}{3}\right) \\ \frac{\sqrt{2}}{2} & \frac{\sqrt{2}}{2} & \frac{\sqrt{2}}{2} \end{bmatrix} \begin{bmatrix} V_a \\ V_b \\ V_c \end{bmatrix} \tag{4}$$

Inverse Park's transformation is:

$$\begin{bmatrix} V_a \\ V_b \\ V_c \end{bmatrix} = \sqrt{\frac{2}{3}} \begin{bmatrix} \cos\theta_r & -\sin\theta_r & \frac{\sqrt{2}}{2} \\ \cos\left(\theta_r - \frac{2\pi}{3}\right) & -\sin\left(\theta_r - \frac{2\pi}{3}\right) & \frac{\sqrt{2}}{2} \\ \cos\left(\theta_r + \frac{2\pi}{3}\right) & -\sin\left(\theta_r + \frac{2\pi}{3}\right) & \frac{\sqrt{2}}{2} \end{bmatrix} \begin{bmatrix} V_d \\ V_q \\ V_0 \end{bmatrix} \tag{5}$$

In (4) and (5), V_{abc} and V_{dq} represents the PMSG stator voltages and $V_0 = 0$. Under balanced conditions, the stator voltage equation of the PMSG in dq-axes reference frame can be expressed as follows [15]

$$V_d = \left(R_g + L_d \frac{d}{dt}\right) i_d - \omega_e L_q i_q \tag{6}$$

$$V_q = \left(R_g + L_q \frac{d}{dt}\right) i_q + \omega_e \psi_{sd} \tag{7}$$

where V_d and V_q are the instantaneous stator voltages in the *dq*-axes reference frame; i_d and i_q are the direct and quadrature stator currents of PMSG in dq frame; L_d and L_q are inductances on the direct and quadrature axis; R_g is resistance of stator; ω_e is the electrical angular speed of the rotor; ψ_{sd} is the stator flux linkage on d-axis.

Stator flux linkages in d and q axis can be written as

$$\psi_{sd} = L_d i_d + \psi_m \tag{8}$$

$$\psi_{sq} = L_q i_q \tag{9}$$

Eqs. (6) and (7) can be rewritten as

$$V_{gd} = R_g i_d + \frac{d}{dt}(\psi_{sd}) - \omega_e(\psi_{sq}) \tag{10}$$

$$V_{gq} = R_g i_q + \frac{d}{dt}(\psi_{sq}) + \omega_e \psi_{sd} \tag{11}$$

Please cite this article in press as: D.K.V. Sagiraju et al., Dynamic performance improvement of standalone battery integrated PMSG wind energy system using proportional resonant controller, Eng. Sci. Tech., Int. J. (2017), http://dx.doi.org/10.1016/j.jestch.2017.03.010

The electrical speed rotation of PMSG is given by

$$\omega = p\omega_m \tag{12}$$

where ω is rotating speed of generator, ω_m is mechanical speed of the generator; p is number of generator pole pairs

The electromagnetic torque of PMSG is given by [7]

$$T_e = 1.5P\left[\psi_{sd} i_q - (L_d - L_q) i_d i_q\right] \tag{13}$$

In permanent magnet machines with the smooth rotor i.e. for surface mounted PMSG, the reluctance is same along d and q axis. On substituting the equal value of d- and q-axis inductances (L_d = - L_q), the electromagnetic torque can be re-written as

$$T_e = 1.5P\psi_{sd} i_q \tag{14}$$

Since, the rotor magnetic flux linkage is constant in PMSG, the electromagnetic torque is directly proportional to quadrature-axis stator current. Hence as evident from (14), the electromagnetic torque in PMSG can be controlled by means of its quadrature-axis current components.

In addition, PMSG active and reactive power are given by [31]

$$P = 1.5\left(V_d i_d + V_q i_q\right) \tag{15}$$

$$Q = 1.5\left(V_q i_d - V_d i_q\right) \tag{16}$$

As the turbine is connected directly to the PMSG, the dynamic equation of the wind turbine is given by:

$$J\frac{d\omega_m}{dt} = T_e - T_m - F\omega_m \tag{17}$$

where F is viscous friction coefficient, Tm is mechanical torque in N-M, Te is generator torque in N-M and J is moment of inertia in ($kg.m^2$)

3. Proposed system and control strategies

3.1. Proposed system

This section is devoted to discuss the proposed system and control strategy. The block diagram of the proposed system is depicted in Fig. 1. The system primarily comprises direct drive PMSG, diode rectifier, DC-DC converter, battery integrated bi-directional DC-DC converter, DC link and inverter. The frequency and voltage at load and machine side are fluctuating owing to variable wind and load conditions. The fluctuating voltage is converted to DC using diode bridge rectifier. Battery interfaced DC-DC bi-directional converter at DC link mainly regulates the DC link voltage variations as well as maintains the power sharing between wind and battery source. The DC voltage at the dc link is converted back to less distorted balanced sinusoidal AC voltage using inverter at the load side.

3.2. Control strategies for the proposed system

The conventional as well as proposed control strategy is discussed in the following subsections.

3.2.1. Conventional vector-PI controller

Fig. 2 shows, the conventional decoupled vector PI controller for load side inverter of standalone PMSG. Load voltage components in synchronous dq reference frame given by [2,3]

$$V_{ld} = Ri_{cd} + L\frac{di_{cd}}{dt} + \omega L i_{cd} + V_{cd} \tag{18}$$

$$V_{lq} = Ri_{cq} + L\frac{di_{cq}}{dt} + \omega L i_{cq} + V_{cq} \tag{19}$$

where R and L are filter Resistance and Inductance respectively; ω is the angular speed of the rotating reference frame; V_{cd}, V_{cq}, V_{ld} and V_{lq} are output voltage of the converter and load on d and q axis respectively.

The dq load voltage components in (18) and (19) are not absolutely dependent owing to the involvement of cross coupled terms $\omega L i_{cd}$ and $\omega L i_{cq}$ .The effect of q-axis on d-axis and vice versa

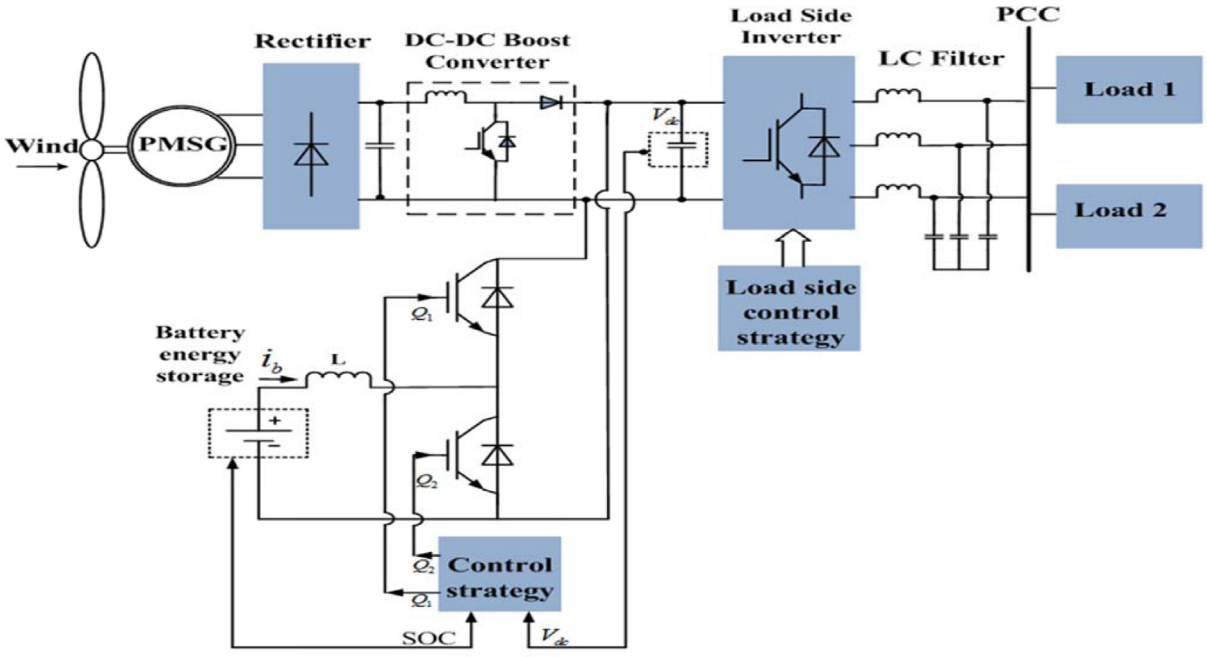

Fig. 1. Block diagram of the proposed system.

Please cite this article in press as: D.K.V. Sagiraju et al., Dynamic performance improvement of standalone battery integrated PMSG wind energy system using proportional resonant controller, Eng. Sci. Tech., Int. J. (2017), http://dx.doi.org/10.1016/j.jestch.2017.03.010

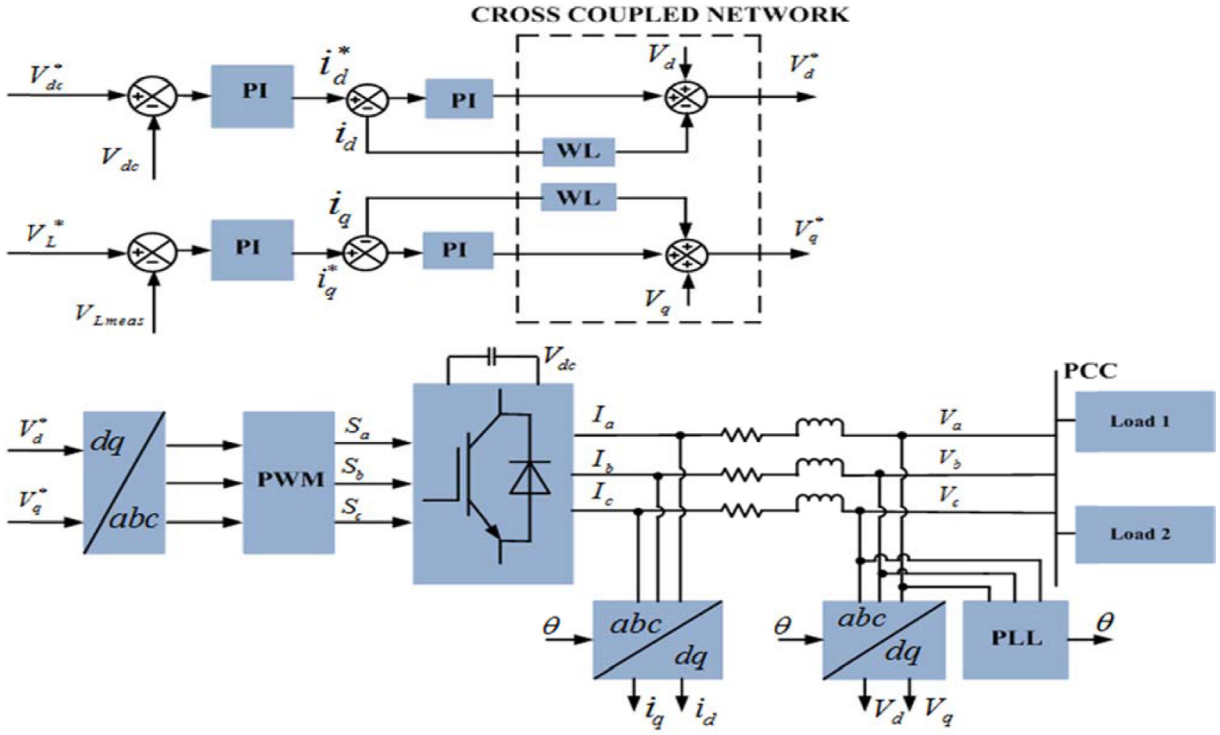

Fig. 2. Decoupled Vector-PI controller.

degrades the performance of the controller. For improving the dynamic performance of the controller, the cross coupling terms are nullified by decoupled network with feed forward signals V_d and V_q as shown in Fig. 2. However, the decoupled network increases the complexity of the system and introduces the delay with many transformations. As shown in Fig. 2, the conventional PI-Vector control uses SRF PLL for extraction of phase angle at PCC voltage. The performance of SRF PLL is not satisfactory under unbalanced load conditions. Further, two separate dq synchronous frame controllers are required to extract the positive and negative sequence components under unbalanced conditions which increases the computational burden which in turn degrades the performance of the system. Hence to overcome the limitations of PI-Vector controller, Proportional Resonant controller is proposed in stationary frame in the subsequent section.

3.2.2. Proposed PR controller strategy

To overcome the disadvantages of conventional vector PI controller, proportional resonant controller is proposed to evaluate the dynamic performance of the system under external disturbances. The PR controller provides a large gain at the fundamental frequency and firmly follows the sinusoidal reference, thus reducing the steady-state error and improving the dynamic performance of the system under external disturbances [35]. The proposed control scheme is realized in single stationary reference frame to compensate both positive and negative sequence components under unbalanced conditions. As a consequence, the computational burden is considerably reduced when compared to PI controller.

The transformation from synchronous dq reference frame to stationary (αβ) reference frame is performed by the following matrix [32].

$$H_{\alpha\beta}(S) = \frac{1}{2}\begin{bmatrix} H^{+}_{dq} + H^{-}_{dq} & JH^{+}_{dq} - JH^{-}_{dq} \\ JH^{+}_{dq} + JH^{-}_{dq} & H^{+}_{dq} + H^{-}_{dq} \end{bmatrix} \tag{20}$$

where

$$H^{+}_{dq} = H_{\alpha\beta}(S + J\omega)$$
$$H^{-}_{dq} = H_{\alpha\beta}(S - J\omega)$$

The equivalent positive sequence controller transfer function for compensating positive sequence component when $H_{dq}(S) = \frac{K_i}{S}$ is

$$H^{+}_{\alpha\beta} = \frac{1}{2}\begin{bmatrix} \frac{2k_{ri}s}{s^2+\omega_r^2} & \frac{2k_{ri}\omega}{s^2+\omega_r^2} \\ -\frac{2k_{ri}\omega}{s^2+\omega_r^2} & \frac{2k_{ri}s}{s^2+\omega_r^2} \end{bmatrix} \tag{21}$$

The equivalent negative sequence controller transfer function for compensating negative sequence component when $H_{dq}(S) = \frac{K_i}{S}$ is

$$H^{-}_{\alpha\beta} = \frac{1}{2}\begin{bmatrix} \frac{2k_{ri}s}{s^2+\omega_r^2} & -\frac{2k_{ri}\omega}{s^2+\omega_r^2} \\ \frac{2k_{ri}\omega}{s^2+\omega_r^2} & \frac{2k_{ri}s}{s^2+\omega_r^2} \end{bmatrix} \tag{22}$$

From (21) and (22), it is noticed that the diagonal terms of the above two equations are same. However, their off diagonal terms are in opposite directions indicating their reversal of direction between positive and negative sequence frames.

Combing the above two equations, the equivalent single stationary reference frame controller for compensating both positive and negative sequence component is expressed in (23) and (24)

$$H_{\alpha\beta}(s) = H^{+}_{\alpha\beta}(s) + H^{-}_{\alpha\beta} \tag{23}$$

$$H_{\alpha\beta}(s) = \frac{1}{2}\begin{bmatrix} \frac{2k_{ri}s}{s^2+\omega_r^2} & 0 \\ 0 & \frac{2k_{ri}s}{s^2+\omega_r^2} \end{bmatrix} \tag{24}$$

The off diagonal terms in the above transfer function matrix are zero indicates that, the cross coupling between alpha and beta signals on stationary reference axis are cancelled. Moreover, the voltage feed forward compensation is also eliminated. Further, under

unbalanced load conditions, the load voltage contains sinusoidal quantities of both positive sequence component and negative sequence component in single stationary reference frame. Hence the PR controller with proper tuning is capable of controlling both the positive and negative sequence currents simultaneously in the stationary reference frame.

The block diagram of PR controller is depicted in Fig. 3.

The transfer function of Proportional Resonant Controller is

$$H_{\alpha\beta}(s) = k_p + \frac{2k_{ri}s}{s^2 + \omega_r^2} \tag{25}$$

where k_p denotes the proportional gain, kri represents the resonant gain and ωr is resonant frequency.

The important feature of PR controller is that it can achieve very high gain close to the resonant frequency and hence, it is capable of eliminating the steady state error between the reference and measured control signal. The dynamic performance of the controller is determined with the proper tuning of its controller parameters. The parameters are adjusted by performing the frequency response analysis. Fig. 4 shows Bode plot of the transfer function of the PR controller given in (25). The magnitude characteristic is plotted with $k_p = 1$, and for different values of integral resonant gains at $\omega_r = 314$ rad/s as shown in Fig. 4. The band width depends on integral gain of the resonant term as shown in Fig. 4. Large value of resonant gain leads to wider bandwidth and small value results in narrow bandwidth. Fig. 4 illustrates that, PR controller with small resonant gain offers very high gain in a narrow frequency band close to the resonant frequency can effectively track the AC signals to reduce the steady state error between measured and reference signal and ensures better dynamic response of the controller.

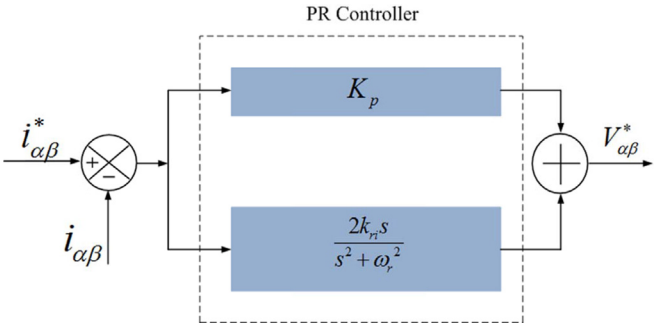

Fig. 3. Block diagram of PR controller.

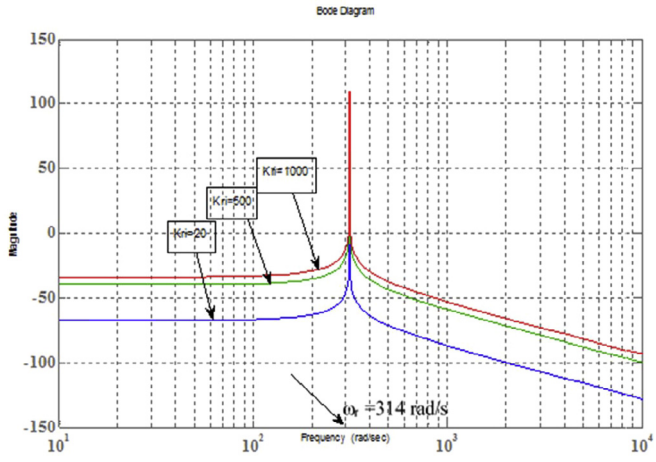

Fig. 4. Bode plot of PR controller.

The proposed control strategy is displayed in Fig. 5. The proposed approach composed of PI controller in the outer voltage loop and proportional resonant controller in the inner loop of load side converter. The phase angle of load voltage is extracted using PLL. The sinusoidal load currents are transformed to stationary αβ signals by abc to αβ transformation. In the outer voltage loop, DC link voltage across the capacitor is compared with reference DC voltage and mismatch is processed by PI regulator to set I_d^*. The reference load voltage is correlated with measured load voltage and mismatch is processed through PI controller to generate I_q^*. The direct and quadrature reference currents are transformed to I_α^* and I_β^* using dq to αβ transformation to control the DC link and load voltage. The stationary reference current signals are given as input to PR controller. The reference current signals are compared with measured current signals which are extracted from abc to αβ transformation are processed through PR controller

$$V^*_{\alpha\beta} = \left(k_p + \frac{2k_{ri}\omega}{s^2 + \omega_r^2}\right)\left(i^*_{\alpha\beta} - i_{\alpha\beta}\right) \tag{26}$$

The PR controller generates stationary voltage reference signals $V_{\alpha\beta}$ and are transformed back to abc voltage components V_{abc} to generate the gate signals for inverter.

3.2.3. Battery energy control strategy for Bi-directional converter for power sharing

The battery energy storage is interfaced to the DC link through bi-directional DC/DC buck-boost converter. The Primary objective of Bi-directional DC-DC converter is to maintain the DC link voltage as well as ensures the power balance between wind and battery to meet the load power. The proposed battery energy control scheme for bi-directional converter is presented in Fig. 6. In this control technique, the outer loop regulates the DC-link voltage by comparing the reference DC link voltage with the actual DC link voltage. The mismatch is processed by PI regulator to set the reference battery current for the inner loop. The battery reference current is compared with original battery current and the mismatch is processed by PI regulator. The PI controller output is passed through PWM (Pulse Width Modulated) generator which generates the gate signals to trigger the upper and lower switches of DC-DC converter to control Power in and out of battery.

When wind power is greater than the load power, the excess power is stored in the DC link. The excess power generated by the wind generator passes through the dc bus, and if any power imbalance occurs, this would appear as a variation in the dc bus voltage. As a result, the DC link voltage as well as the current flowing through battery increases. The reference battery current set by the outer voltage loop is compared with the current flowing through battery and the error is processed through PI regulator. Based on the error signal, the PI controller generates the appropriate value to generate a suitable pulse-width modulation (PWM) signal for the switches. In this scenario, the upper switch Q1 is turned ON and the lower switch Q2 is turned OFF with diode D1, D2 reverse biased as shown in Fig. 7. During this interval, the converter operates in buck mode and transfer power to the battery bank. In this context, bi directional converter acts as buck converter and the battery moves into charged mode of operation.

When the wind power is less than the load power, less energy is accumulated in the DC link. Hence, the DC link voltage and current flowing through the battery decreases. The current flowing through the battery is compared with reference battery current. The error is processed by the PI regulator. Based on PI controller output, the PWM generator generates the gate signals for switches in the bi-directional converter. In this scenario, the lower switch Q2 is turned ON and the upper switch Q1 is turned OFF with diode D1, D2 reverse biased as shown in Fig. 8. The inductor gets fully

Please cite this article in press as: D.K.V. Sagiraju et al., Dynamic performance improvement of standalone battery integrated PMSG wind energy system using proportional resonant controller, Eng. Sci. Tech., Int. J. (2017), http://dx.doi.org/10.1016/j.jestch.2017.03.010

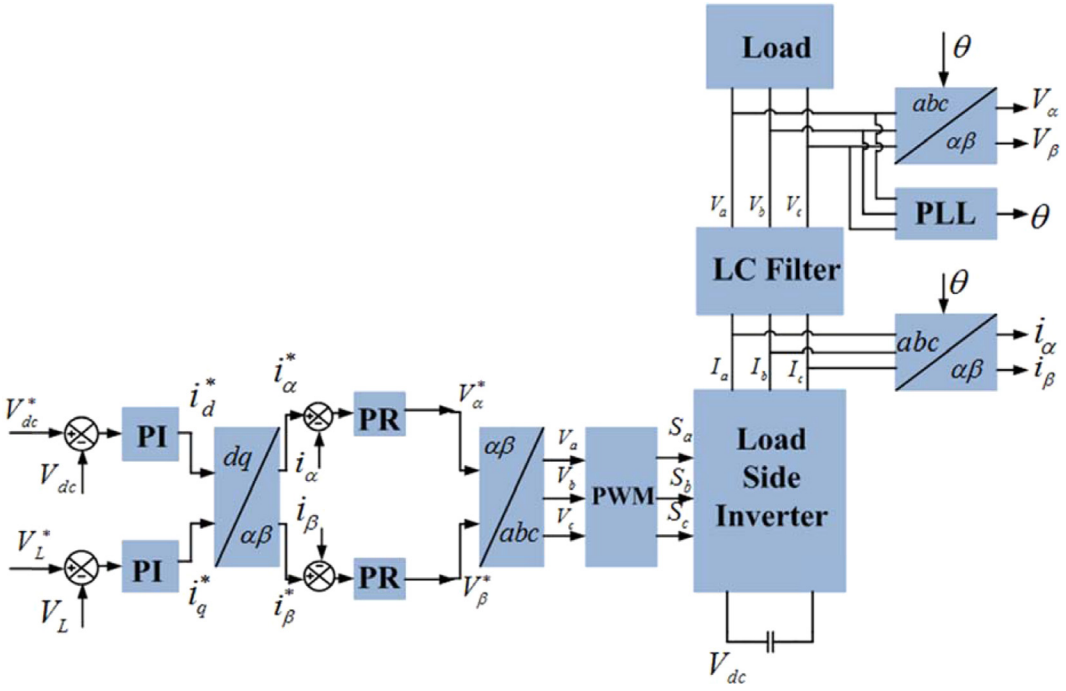

Fig. 5. Proportional resonant controller strategy.

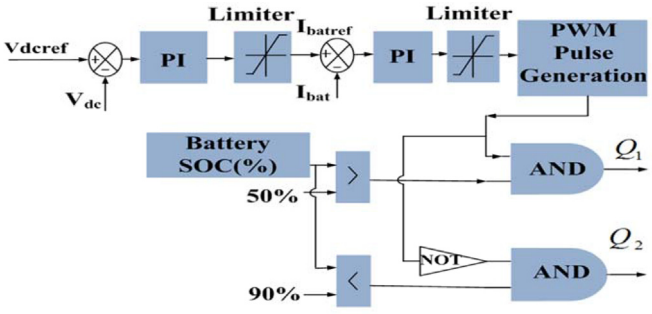

Fig. 6. Battery Energy Controller.

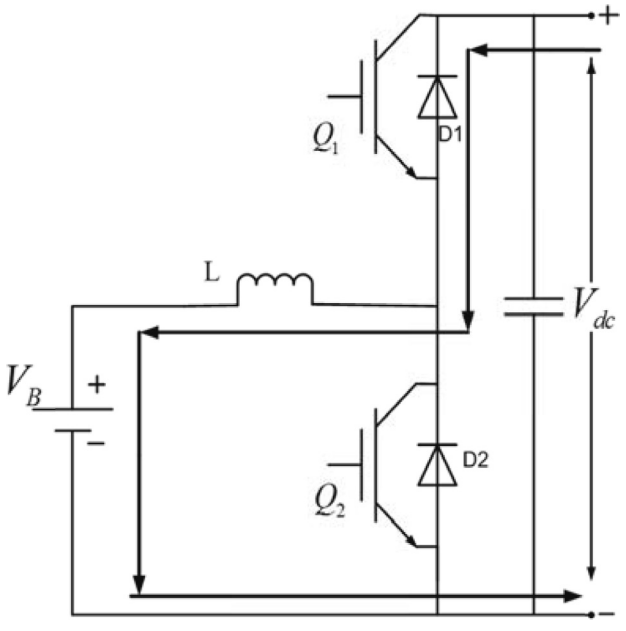

Fig. 7. Bi-directional DC/DC converter in buck mode.

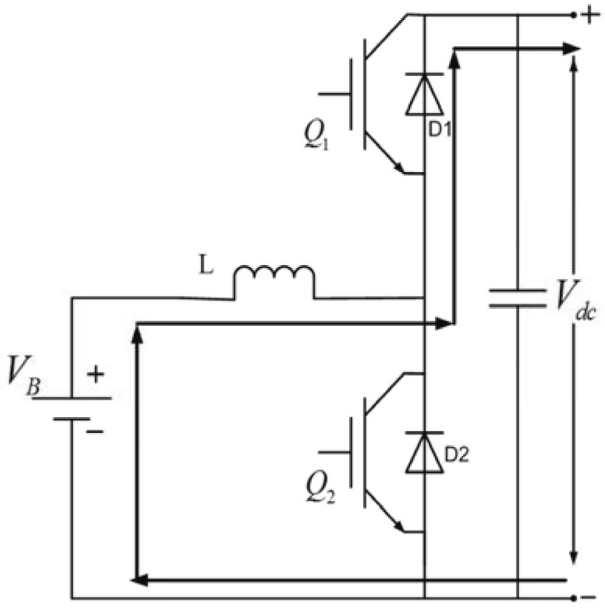

Fig. 8. Bi-directional DC/DC converter in boost mode.

charged initially. Once the inductor gets fully charged, the switches Q2 and Q1 are turned off. The diode D1 of the upper switch Q1 starts conducting as shown in Fig. 8. The converter in this case Supplies power to the DC-link voltage. During this time, the converter operates in boost mode and the battery moves into discharged mode of operation

The charging and discharging conditions of the battery are dependent on State of Charge (SOC). In the proposed battery control scheme, when battery SOC exceeds 50%, BESS (Battery Energy Storage System) delivers the deficit power to load. When the SOC is less than 90%, then the battery absorbs the excess power and operates in charging mode.

Please cite this article in press as: D.K.V. Sagiraju et al., Dynamic performance improvement of standalone battery integrated PMSG wind energy system using proportional resonant controller, Eng. Sci. Tech., Int. J. (2017), http://dx.doi.org/10.1016/j.jestch.2017.03.010

4. Simulation results and discussion

The proposed system has been simulated in MATLAB/SIMULINK environment. The following cases are considered to investigate the performance of standalone direct drive PMSG using the proposed control method. The results accomplished through the proposed control are compared with the conventional vector control.

4.1. Dynamic performance improvement of PMSG under variable wind and load conditions: (Increase in wind velocity and step change in linear balanced load condition)

The fluctuating load and variable wind variation is considered to assess the performance of standalone PMSG. Wind velocity shown in Fig. 9(a) is initially set at 8 m/s and it changes from

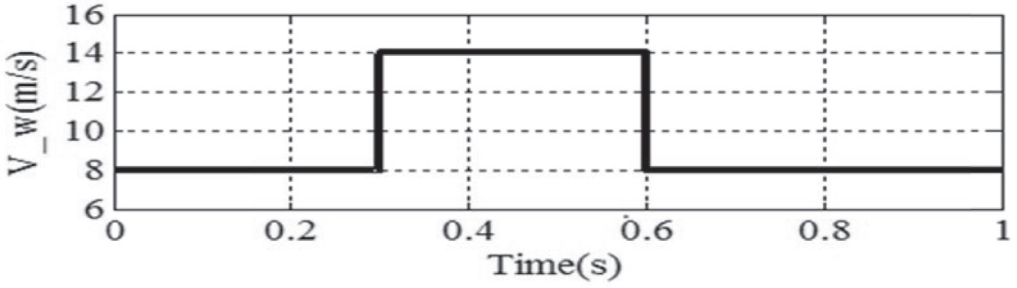

(a) Wind velocity

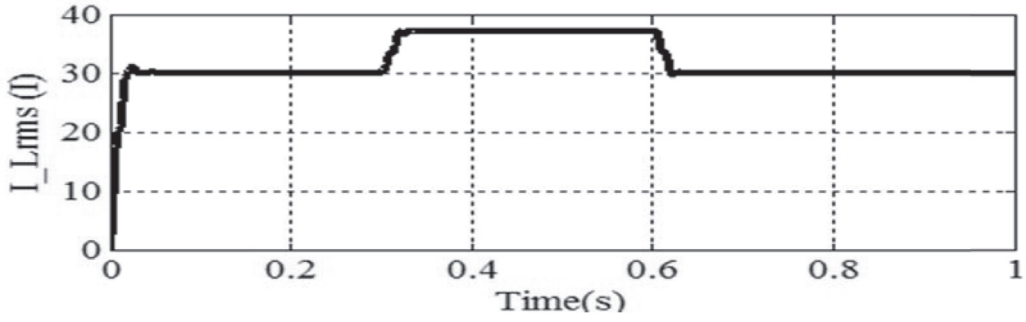

(b) Load current

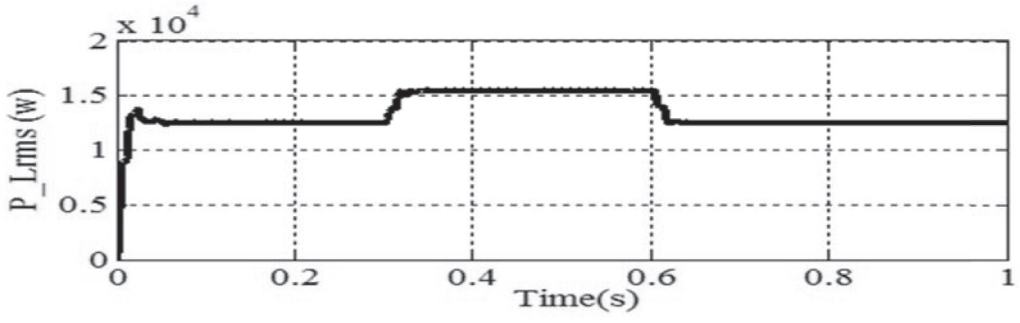

(c) Load Power

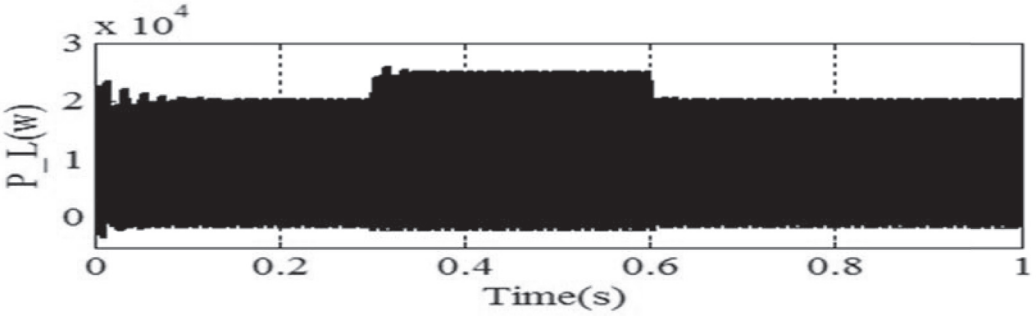

(d) Wind Power

Fig. 9. Variable wind with increase in wind velocity and variable load condition.

Please cite this article in press as: D.K.V. Sagiraju et al., Dynamic performance improvement of standalone battery integrated PMSG wind energy system using proportional resonant controller, Eng. Sci. Tech., Int. J. (2017), http://dx.doi.org/10.1016/j.jestch.2017.03.010

8 m/s to 14 m/s at t = 0.3 s. The load switching with step increase and decrease in load has been considered at t = 0.3 s and t = 0.6 s. The corresponding increase in load current, load power and wind power are depicted in Fig. 9(b–d).

The deviation in wind and load will influence the load voltage, frequency, dc link voltage and PMSG parameters. The simulation results using conventional vector control and proposed control strategy are shown in Fig. 10(a–e). The effectiveness of proposed control strategy to sustain the voltage and frequency within the bounds is confirmed from Fig. 10(a) and (b). The DC link voltage depicted in Fig. 10(c) is also well regulated and stays within ±5% of rated value regardless of wind and load variations. As a result

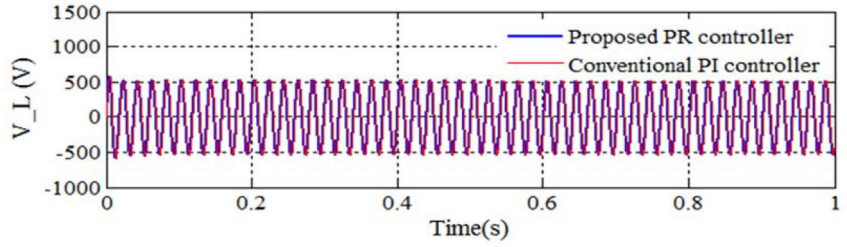

(a) Load voltage

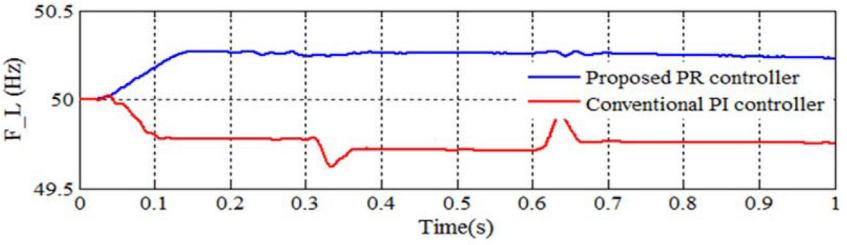

(b) Frequency of load voltage

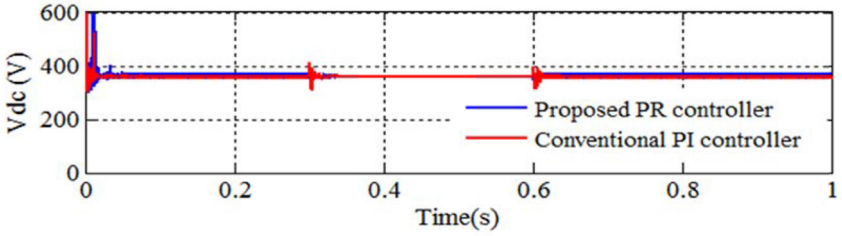

(c) DC link voltage

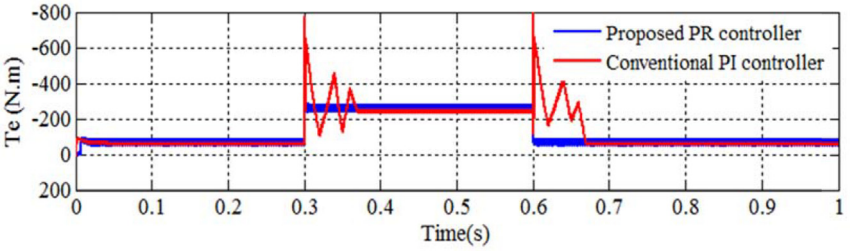

(d) Electromagnetic torque

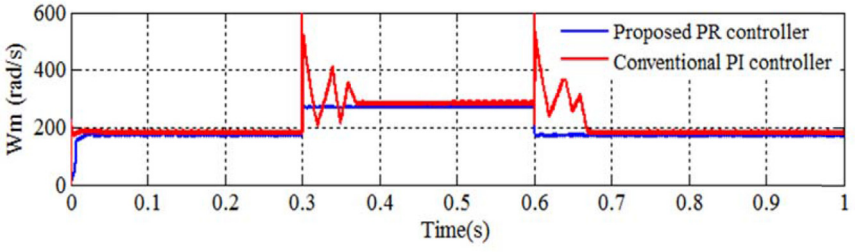

(e) Rotor speed

Fig. 10. Simulation results varying wind and balanced load conditions.

Please cite this article in press as: D.K.V. Sagiraju et al., Dynamic performance improvement of standalone battery integrated PMSG wind energy system using proportional resonant controller, Eng. Sci. Tech., Int. J. (2017), http://dx.doi.org/10.1016/j.jestch.2017.03.010

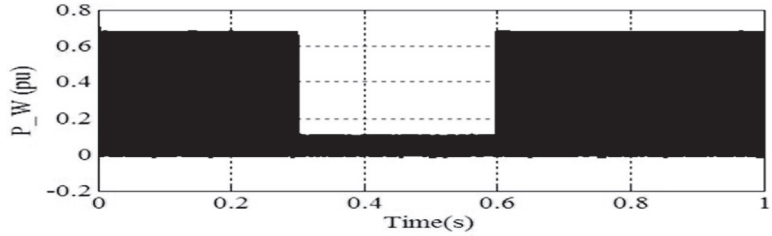

(a) Wind Power

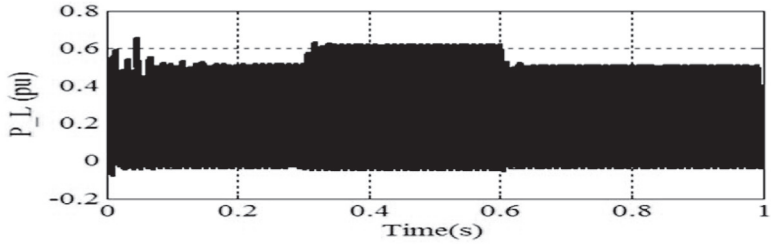

(b) Load Power

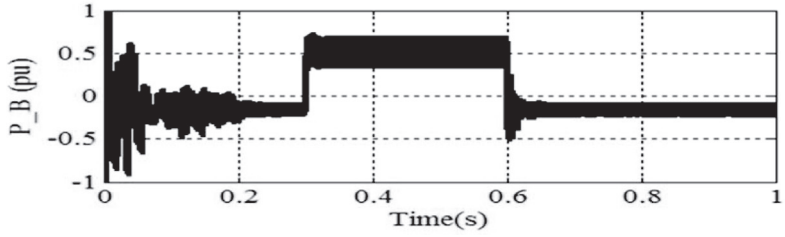

(c) Battery power

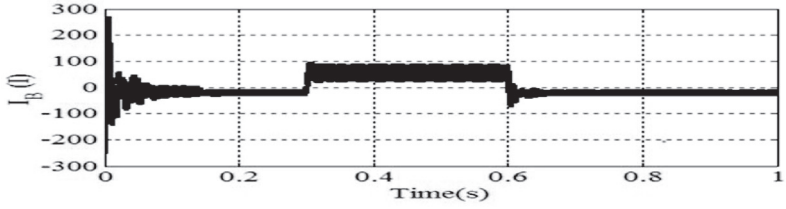

(d) Battery current

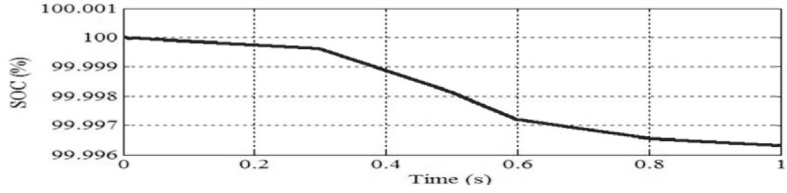

(e) State of charge of battery

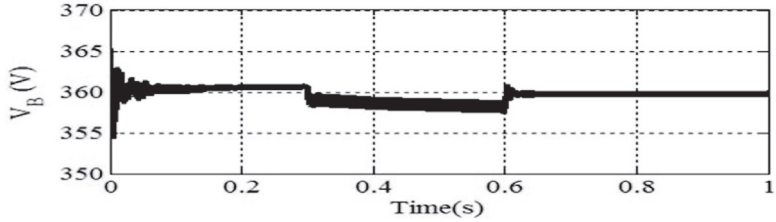

(f) Battery voltage

Fig. 11. Simulation results for Power management for variable wind (low wind velocity) and variable load conditions.

Please cite this article in press as: D.K.V. Sagiraju et al., Dynamic performance improvement of standalone battery integrated PMSG wind energy system using proportional resonant controller, Eng. Sci. Tech., Int. J. (2017), http://dx.doi.org/10.1016/j.jestch.2017.03.010

of increase in wind speed, the respective increase in electromagnetic torque and rotor speed are seen in Fig. 10(d) and (e). Fig. 10(d)–(e) illustrate that there is less variation in electromagnetic torque and rotor speed under varying wind and load condition. The proposed method implemented in stationary reference frame offers very high gain around the resonant frequency with proper selection of resonant gain. Hence the proposed method is capable of tracking the sinusoidal signals easily and eliminating the steady state error in the control and reference signal. Therefore with the proposed control strategy, the steady state error in load and machine parameters can be greatly reduced as shown in Fig. 10. In contrast, the classical PI controller has been implemented in dq reference frame with cross coupling terms between d and q axis. Hence, the Vector- PI controller cannot track sinusoidal signals and could not eliminate the steady state error. Further, the cross coupling effect between d and q axis deteriorates the performance of PI controller. Hence, large variations in load and machine parameters is seen in Fig. 10.

The power sharing of PMSG Battery energy system under unstable wind (decrease in wind) and variable load condition is shown in Fig. 11. At t = 0.3 s, the drop in wind speed and increase in real power load creates the mismatch in generation and load balance

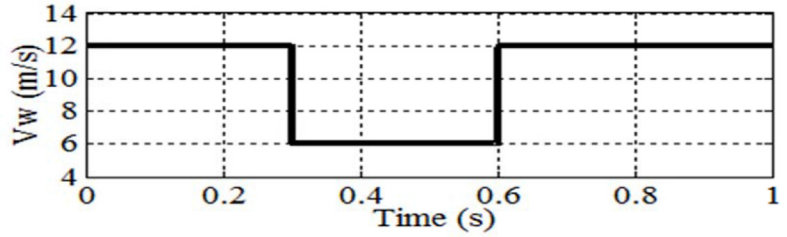

(a) Decrease in wind velocity

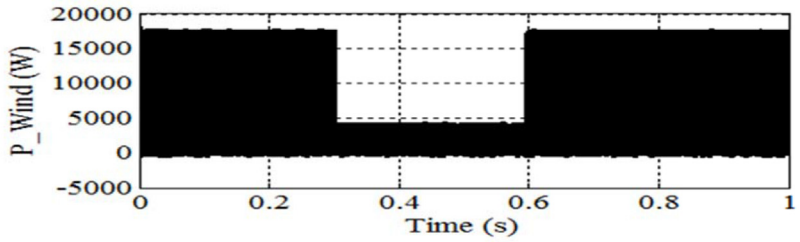

(b) Wind Power

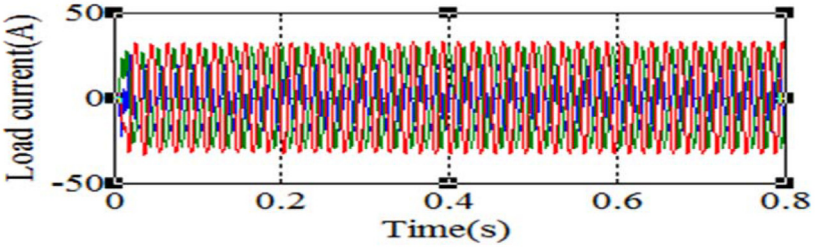

(c) Unbalanced Load current

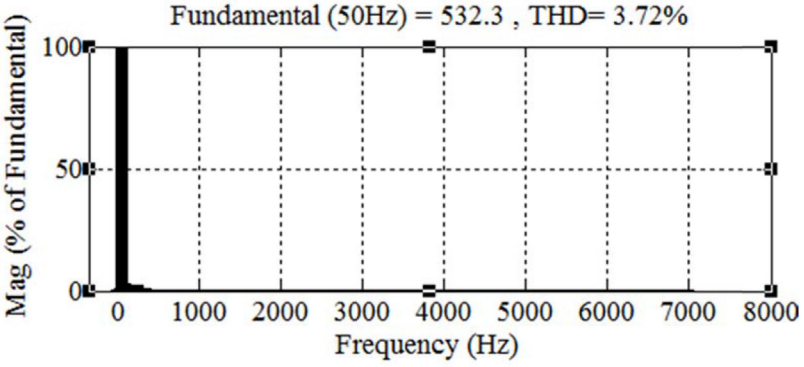

(d) FFT analysis of Load current

Fig. 12. Variable wind with drop in wind velocity and unbalanced load condition.

Please cite this article in press as: D.K.V. Sagiraju et al., Dynamic performance improvement of standalone battery integrated PMSG wind energy system using proportional resonant controller, Eng. Sci. Tech., Int. J. (2017), http://dx.doi.org/10.1016/j.jestch.2017.03.010

leads to under generation. Due to insufficient power generation at low wind speeds, the wind power could not supply enough power. The reduction in wind power output is depicted in Fig. 11(a). The increase in load power due to step increase in load is shown in Fig. 11(b). The battery delivers deficit power to meet the increase in load demand at t = 0.3 s as seen in Fig. 11(c). At t = 0.3 s, the battery changes its mode of operation from charging to discharging mode. The load shedding at t = 0.6 s, creates mismatch between generation and load leads to over generation. At t = 0.6 s, the battery changes its mode of operation from discharging mode to charging mode as shown in Fig. 11(d) to ensure stable supply of load. The state of charge of the battery slightly decreases and

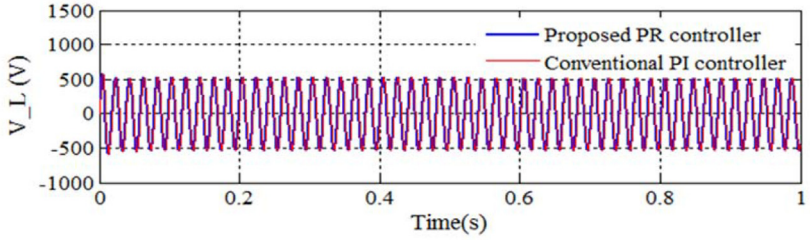

(a) Load votage

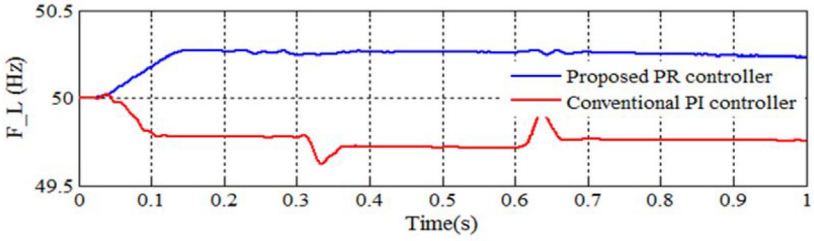

(b) Frequency of load voltage

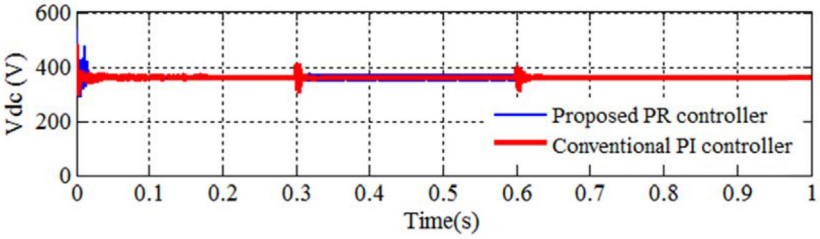

(c) DC link voltage

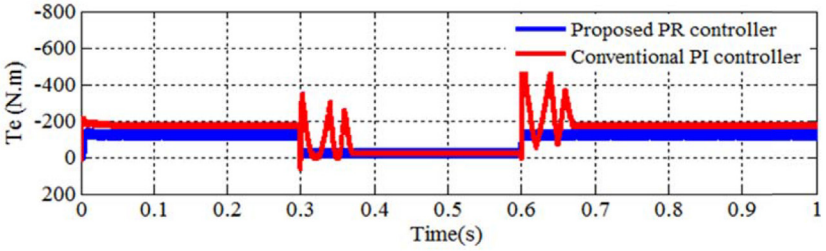

(d) Electromagnetic torque

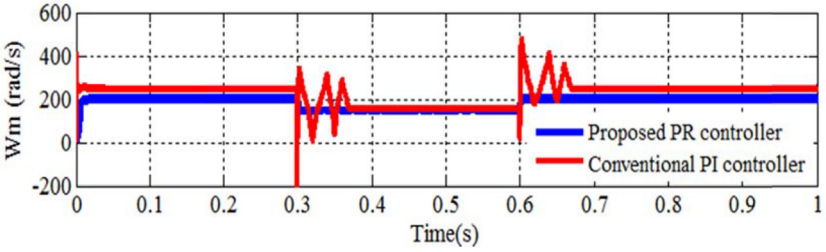

(e) Rotor speed

Fig. 13. Simulation results under Variable wind and unbalanced load conditions.

Please cite this article in press as: D.K.V. Sagiraju et al., Dynamic performance improvement of standalone battery integrated PMSG wind energy system using proportional resonant controller, Eng. Sci. Tech., Int. J. (2017), http://dx.doi.org/10.1016/j.jestch.2017.03.010

increases when change in wind and load occur as shown in Fig. 11 (e). Fig. 11(f) shows that, the battery voltage slightly decreases by small amount during charging period at t = 0.3 s and increases during discharging period at t = 0.6 s. The proposed control strategy ensures the power sharing to maintain reliable supply to the loads under variable wind and load conditions.

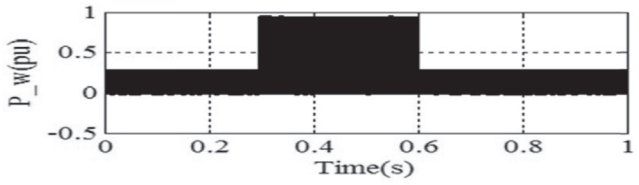

(a) Wind power

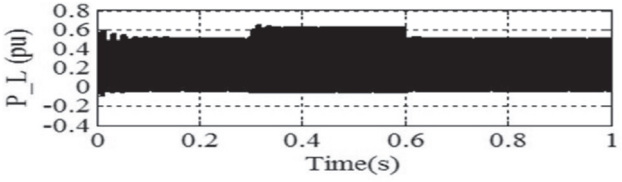

(b) Load Power

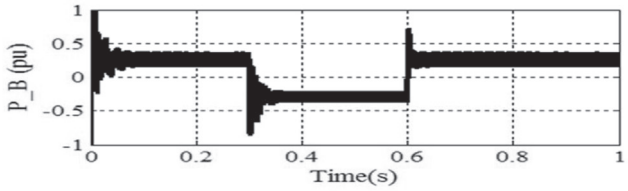

(c) Battery power

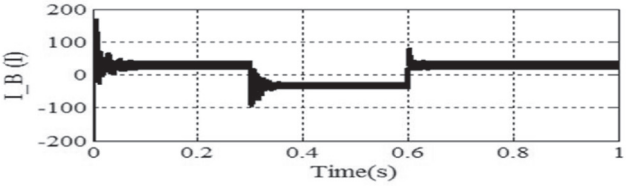

(d) Battery current

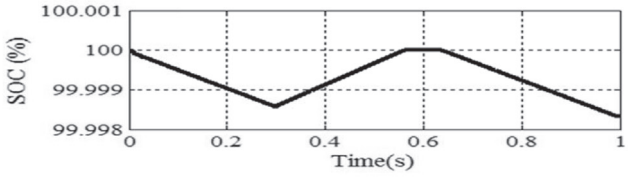

(e) State of charge of battery

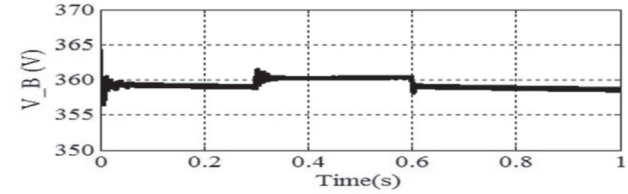

(f) Battery voltage

Fig. 14. Simulation results for Power management for variable wind (High wind velocity) and variable load conditions.

4.2. Dynamic performance improvement of PMSG under variable wind with unbalanced load conditions (decrease in wind velocity and unbalanced load condition)

The variable wind with drop in wind velocity from 12 m/s to 6 m/s is considered at t = 0.3 s as portrayed in Fig. 12(a). The corresponding wind power due to decrease in wind velocity is shown in Fig. 12(b). The unbalanced load current is depicted in Fig. 12(c). Due to the negative sequence component of load current under unbalanced load condition, the load current contains some harmonic component. The FFT (Fast Fourier Transform) analysis has been performed to show the percentage of harmonic present in the load current. The harmonic component of load current is depicted in Fig. 12(d).

The simulation results using PR and PI control strategy are shown in Fig. 13(a–e). From Fig. 13(a–e), it is evident that, the effect of unbalanced load causes pulsating oscillations in load frequency, electromagnetic torque, rotor speed and DC link voltage which will reduce the life of the turbine shaft. Under unbalanced load conditions, the load current contains sinusoidal quantities of both positive and negative sequence component in single stationary reference frame. The proposed method with proper tuning of PR control parameters is capable of controlling both the positive and negative sequence currents simultaneously in single stationary reference frame. Hence, from Fig. 13(a–e), it can be noticed that, the pulsating pulsations in frequency, dc-link voltage, electromagnetic torque and rotor hub speed are minimized under unbalanced load conditions.

The power sharing of PMSG Battery energy system under unstable wind (increase in wind) and variable load condition is shown in Fig. 14. The increase in wind speed and load at t = 0.3 s creates mismatch between generation and load leads to over generation. The corresponding increase in wind and load power is illustrated in Fig. 14(a) and Fig. 14(b). Due to increase in wind velocity at t = 0.3 s, the battery transits its mode of operation from discharging to charging mode due to excess wind generation. Hence, battery current and power delivered by battery is reduced at t = 0.3 s, as shown in Fig. 14(c) and Fig. 14(d). The drop in wind velocity and the load connection at t = 0.6 s creates mismatch between generation and load leads to under generation. Hence, at t = 0.6 s, due to deficit wind power the battery moves from charging to discharging mode to meet the load demand. As a result, battery current and power delivered by battery increases at t = 0.6 s, as shown in Fig. 14(c) and (d). Fig. 14(e) illustrates that, the battery state of charge (SOC) changes with battery charge/discharge condition to ensure power balance in the system. Fig. 14(f) shows that, the battery voltage slightly increases by small amount during charging period at t = 0.3 s and decreases during discharging period at t = 0.6 s. From simulation results it is shown that, the proposed battery energy controller acts as an auxiliary source to maintain power management in the system.

5. Conclusion

This paper has presented a coordinated proportional resonant and battery energy controller to improve power quality and power management in standalone battery integrated PMSG wind energy system. The robustness of the proposed controller to improve the dynamic performance of PMSG is demonstrated under various operating conditions. The simulation results have demonstrated that, the proposed control scheme shows good dynamic performance under variable wind and load conditions. The effectiveness of the proposed control strategy is validated by comparing with the conventional vector control strategy using MATLAB/SIMULINK environment. From the results, it is seen that, the proposed battery

Please cite this article in press as: D.K.V. Sagiraju et al., Dynamic performance improvement of standalone battery integrated PMSG wind energy system using proportional resonant controller, Eng. Sci. Tech., Int. J. (2017), http://dx.doi.org/10.1016/j.jestch.2017.03.010

energy control scheme also ensures the power management between battery and wind to meet the load demand under variable wind and load conditions.

Acknowledgement

The authors gratefully acknowledge the support provided by Shri Vishnu Engineering College for Women, Bhimavaram.

Appendix A

Simulation parameters	Values
PMSG Rated Power	40 KW
PMSG Rated Voltage	595 V
PMSG Stator Resistance Rs	1.8750 pu
Direct Inductance	0.085 (mh)
Quadrature Inductance	0.085 (mh)
Machine Inertia	0.3 (J kg-m^2)
Number of pole pairs	4
rotor speed	200 rpm
DC link Voltage	1200
DC link capacitance	20 mF
Operating Wind speed	12 m/s
Battery Rated Capacity (amp-h)	160
Rated voltage of battery (V)	360
PI controller parameters	$K_p = 12$, $K_i = 0.1$
PR controller parameters	$K_p = 1$, $K_{ri} = 20$

References

[1] L. Barote, C. Marinescu, M.N. Cirstea, Control structure for single-phase stand-alone wind-based energy sources, IEEE Trans. Ind. Electron. 60 (2013) 764–772.
[2] B. Bahrani, A. Karimi, B. Rey, A. Rufer, Decoupled dq-current control of grid-tied voltage source converters using nonparametric models, IEEE Trans. Ind. Electron. 60 (2013) 1356–1366.
[3] B. Bahrani, S. Kenzelmann, A. Rufer, Multivariable-PI-based dq current control of voltage source converters with superior axis decoupling capability, IEEE Trans. Ind. Electron. 58 (2011) 3016–3026.
[4] J. Chen, W. Zhang, B. Chen, Y. Ma, Improved vector control of brushless doubly fed induction generator under unbalanced grid conditions for offshore wind power generation, IEEE Trans. Energy Convers. 31 (2016) 293–302.
[5] J. Chen, C. Gong, On optimizing the aerodynamic load acting on the turbine shaft of PMSG-based direct-drive wind energy conversion system, IEEE Trans. Ind. Electron. 61 (2013) 4022–4031.
[6] Y. Errami, M. Maaroufi, M. Ouassaid, A MPPT vector control of electric network connected Wind Energy Conversion System employing PM Synchronous Generator, in: International Renewable and Sustainable Energy Conference (IRSEC), Ouarzazate, 2013, pp. 228–233.
[7] Y. Errami, M. Maaroufi, C. Maaroufi, M. Maaroufi, Variable structure sliding mode control and direct torque control of wind power generation system based on the PM synchronous generator, J. Electr. Eng. 66 (2015) 121–131.
[8] A.E. Fitzgerald, C. Kingsley, S.D. Umans, Electric machinery, sixth ed., McGraw-Hill, Boston, 2003.
[9] Lijun He, Yongdong Li, R.G. Harley, Adaptive multi-mode power control of a direct-drive PM wind generation system in a micro grid, IEEE J. Emerg. Sel. Top. Power Electron. 1 (2013) 217–225.
[10] M.E. Haque, K.M. Muttaqi, M. Negnevitsky, Control of a standalone variable speed wind turbine with a permanent magnet synchronous generator, in: IEEE Power and Energy Society General Meeting - Conversion and Delivery of Electrical Energy in the 21st Century, Pittsburgh, PA, July, 2008.
[11] M.E. Haque, M.K. Negnevitsky, M.A. Muttaqi, Novel control strategy for a variable-speed wind turbine with a permanent-magnet synchronous generator, IEEE Trans. Ind. Electron. 46 (2010) 331–339.
[12] N.K. Jena, K.B. Mohanty, H. Pradhan, S.K. Sanyal, A decoupled control strategy for a grid connected direct-drive PMSG based variable speed wind turbine system, in: International Conference on Energy, Power and Environment: Towards Sustainable Growth (ICEPE), Shillong, 2015, pp. 1–6.
[13] H. Nian, Y. Song, Optimized parameter design of proportional integral and resonant current regulator for doubly fed induction generator during grid voltage distortion, IET Renewable Power Gener. 8 (2014) 299–313.
[14] M. Kassem, S.A. Zaid, Load parameter waveforms improvement of a stand-alone wind-based energy storage system and Takagi-Sugeno fuzzy logic algorithm, IET Renewable Power Gener. 8 (2014) 775–785.
[15] P. Krause, O. Wasynczuk, S. Sudhoff, S. Pekarek, Analysis of Electric Machinery and Drive Systems, 3rd ed., IEEE Press, Wiley Hoboken, NJ, USA, 2013.
[16] C. Liu, K.T. Chau, X. Zhang, An efficient wind–photovoltaic hybrid generation system using doubly excited permanent-magnet brushless machine, IEEE Trans. Ind. Electron. 57 (2010) 831–839.
[17] N. Lachguer, M.T. Lamchich, Control strategy of permanent magnet synchronous generator for standalone wind power generation system, in: International Aegean Conference on Electrical Machines and Power Electronics and Electro Motion, Istanbul, 2011, pp. 392–397.
[18] C. Liu, F. Blaabjerg, W. Chen, D. Xu, Stator current harmonic control with resonant controller for doubly fed induction generator, IEEE Trans. Power Electron. 27 (2012) 3207–3220.
[19] M. Mahmud Hussein, S. Tomonobu, A. Orabi Mohamed, M. Hamada, Control of a stand-alone variable speed wind energy supply system, J. Appl. Sci. 3 (2013) 437–456.
[20] N. Mendis, K.M. Muttaqi, S. Sayeef, S. Perera, A control approach for voltage and frequency regulation of a Wind-Diesel-battery based hybrid remote area power supply system, in: 36th Annual Conference of the IEEE Industrial Electronics Society, 2010, pp. 3054–3060.
[21] N. Mendis, K.M. Muttaqi, S. Sayee, S. Perera, Operation of wind turbine-based variable speed generators with maximum power extraction capability, IEEE Trans. Energy Converse. 27 (2012) 822–834.
[22] N. Mendis, K.M. Muttaqi, S. Sayeef, Management of battery-super capacitor hybrid energy storage and synchronous condenser for isolated operation of PMSG based variable-speed wind turbine generating systems, IEEE Trans. Smart Grid 5 (2014) 944–953.
[23] H. Nian, R. Zeng, Improved control strategy for stand-alone distributed generation system under unbalanced and non-linear loads, IET Renewable Power Gener. 5 (2011) 323–331.
[24] O. Onur, M. Ismail, A. Hakk, Fuzzy logic control for a wind/battery renewable energy production system, Turk. J. Elec. Eng. Comp. Sci. 20 (2012) 187–205.
[25] R. Pena, R. Cardenas, E. Escobar, J. Clare, P. Wheeler, Control system for unbalanced operation of stand-alone doubly fed induction generators, IEEE Trans. Energy Convers. 22 (2007) 544–545.
[26] R. Pena, R. Cardenas, E. Escobar, J. Clare, P. Wheeler, Control strategy for a Doubly-Fed Induction Generator feeding an unbalanced grid or stand-alone load, Electric Power Systems Research 79 (2009) 355–364.
[27] V.T. Phan, H. Lee, Elimination of voltage harmonics in a stand-alone DFIG using a PI-R controller in the fundamental reference frame, in: IEEE International Conference on Sustainable Energy Technologies (ICSET), Kandy, December, 2010.
[28] V.T. Phan, H. Lee, Control strategy for harmonic elimination in stand-alone DFIG applications with nonlinear loads, IEEE Trans. Power Electron. 26 (2011) 2662–2675.
[29] V.T. Phan, H. Lee, Performance enhancement of stand-alone DFIG systems with control of rotor and load side converters using resonant controllers, IEEE Trans. Ind. Appl. 48 (2012) 199–210.
[30] M. Rezkallah, A. Chandra, B. Singh, M. El Kahel, Vector control of squirrel-cage induction generator for stand-alone wind power generation, in: 38th Annual IEEE Industrial Electronics Society conference, Montreal, QC, October, 2012.
[31] S. Zhang, K. Tseng, B. Mahindra Vilathgamuwa, T. Nguyen, X. Wang, Design of a robust grid interface system for PMSG-based wind turbine generators, IEEE Trans. Ind. Electron. 58 (2011) 316–328.
[32] R. Teodorescu, F. Blaabjerg, U. Borup, M.A. Liserre, New control structure for grid-connected LCL PV inverters with zero steady-state error and selective harmonic compensation, in: Nineteenth Annual IEEE Applied Power Electronics Conference and Exposition, vol. 1, 2004, pp. 580–586.
[33] F. Wei, D.M. Vilathgamuwa, S. Choi, X. Zhang, Improved control of rotor- and load-side converters of stand-alone DFIGs under nonlinear loads conditions, in: IEEE ECCE Asia Conference, Melbourne, June 2013.
[34] H. Zeng, Y. Nian, J. Quan, J. Liu, Improved load-adaptive control strategy for PMSG based stand-alone wind energy generation system, in: IEEE International Conference on Electrical Machines and Systems, Tokyo, November 2009.
[35] D.N. Zmood, D.G. Holmes, Stationary frame current regulation of PWM inverters with zero steady-state error, IEEE Trans. Power Electron. 18 (2003) 814–822.

Please cite this article in press as: D.K.V. Sagiraju et al., Dynamic performance improvement of standalone battery integrated PMSG wind energy system using proportional resonant controller, Eng. Sci. Tech., Int. J. (2017), http://dx.doi.org/10.1016/j.jestch.2017.03.010